Received: 25 June 2019 | Revised: 9 August 2019 | Accepted: 12 September 2019

DOI: 10.1111/jfpe.13281

ORIGINAL ARTICLE

Journal of Food Process Engineering WILEY

A roll-type corona discharge–electrostatic separator for separating wheat grain and straw particles

Mohammad Jafari[1,2] | Gholamreza Chegini[1] | Amir A. Shayegani Akmal[3] | Behrooz Rezaeealam[4]

[1]Department of Agrotechnology, College of Abouraihan, University of Tehran, Tehran, Iran

[2]Agriculture Research Education and Extension ORG, Research Institute in Tehran, Tehran, Iran

[3]Electrical Faculty of Tehran University, Tehran, Iran

[4]Electrical Engineering Department, Lorestan University, Lorestan, Iran

Correspondence
Gholamreza Chegini, Department of Agrotechnology, College of Abouraihan, University of Tehran, Tehran, Iran.
Email: chegini@ut.ac.ir

Abstract

Different methods such as mechanical, pneumatic, and electrical techniques have been used in the separation process of impurities from agricultural products. In electrical systems, three methods, that is, triboelectrostatic, free fall, and roll type with high-voltage corona discharge electrodes, are usually used. In the present study, separation trajectory of grain and wheat straw are firstly predicted using simulation of roll-type corona system configuration in COMSOL Multiphysics and MATLAB. Experimental tests are conducted to determine the separation performance of a roll-type corona apparatus with 10, 15, 20, 25, and 30 kV voltages at 50, 70, and 90 rpm drum rotational speeds. The simulation results showed that the trajectory of the grain particles deviated from that of straw when the voltage increased from 10 to 30 kV as well as increasing the rotational speed from 50 to 90 rpm. Although the rotational speed of 70 rpm resulted in a good separation of grains from straw particles, increasing the speed to 90 rpm not only did not improve the separation performance but also caused a dispersal of the particles and reduced the separation quality. The simulation results were in good accordance with the experimental results obtained from the developed prototype.

Practical applications: The results of this study can be used in configuration optimization design of "Corona Type Cylindrical Electrostatic Separation" for separating seed and straw in agriculture production, especially where they cannot be separated by conventional methods.

1 | INTRODUCTION

Seeds harvested from a farm often have various impurities such as waste, weed seeds, stem, leaves, and damaged seeds. Some seeds are completely cleansed after an initial cleaning process and become the final product. However, in others, additional operations are required to remove impurities (Miller & Copeland, 1997). Seed separation is one of the important processes in obtaining pure high-quality seeds. Many types of seeds can be completely cleaned using sieve cleaning. In other cases, however, further operations may be desirable or necessary to remove specific contaminants (Miller & Copeland, 1997).

Wheat is one of the most important human food elements and its function highly depends on seed quality. Seed quality is achievable under practical drying conditions to reach the desired moisture, cleaning to remove impurities, and refining to remove wrinkled grains (Butunoi et al., 2011). Traditional mechanical separators have the capability of separating grains according to their geometric characteristics and weights, such as width, length, and thickness (Rawa & Kaliniewicz, 1998). However, when the impurities of the product, such as shriveled and broken seeds, are dimensionally similar to the original grains, it will be necessary to use wind turbines with segregated plates with different wind currents (Drintcha & Pavlov, 2002). Therefore,

their separation requires a knowledge on their electrical properties. For more effective separation of undesirable seeds, a combination of electrical and mechanical methods should be used (Kazimirchuk & Xziretdinov, 1995; Požėlienė & Lynikienė, 1998). One of the separating methods that is used extensively for separating small particles of dry material is electrostatic separation (Mortezapour, Moshirirad, & Akhbari, 2015), which is based on the attractive and repulsive forces among charged particles in a very strong electric field, which, in addition to the electrical conductivity of the particles, depends on their moisture contents (Harmond, Brandenburg, & Klein, 1968). For this reason, electrostatic separation is also called high-tension separation (Ralston, 1961). In this method, particles become electrically charged. Then, during passing through an electric field, they become influenced by several forces, such as electricity and gravity, and pass different paths based on their size, density, and electrical conductivity (Li, Ban, Hower, Stencel, & Saito, 1999).

The application of this method is in minerals, agricultural seeds, food industry, and recycling. In other words, the electrostatic separator is an equipment for the separation of charged and dipolar solids by electrical forces (Reguig et al., 2017). The electrical separation process is the result of a balance between electrical forces and other mechanical forces. It is difficult to obtain a precise theoretical model illustrating the performance of all forces. Therefore, the application of an empirical method is the only way to optimize the separation conditions (Remadnia et al., 2014; Messal, Zeghloul, Benhafssa, & Dascalescu, 2016). More recent research has investigated electrostatic fractionation of solids. Electrostatic separation has been studied for the recovery of valuable materials from spent lithium-ion batteries (Silveira, Santana, Tanabe, & Bertuol, 2017). This method relies on differences in the dielectric properties of feed particles instead of differences in their size and density (Assatory, Vitelli, Rajabzadeh, & Legge, 2019). The principle underlying electrostatic separation is that for protein/starch mixtures, the proteins can be charged to a much higher extent than carbohydrates due to the presence of ionizable groups in their amino acid residues, N terminus and C terminus (Tabtabaei, Jafari, Rajabzadeh, & Legge, 2016). Thus, an electric field can separate protein-rich and carbohydrate-rich particles according to their differing types and magnitudes of charge (Assatory et al., 2019). The charging behavior of flour is species dependent, as protein bodies from flours of different origins exhibit different shapes, sizes, and surface properties (Pelgrom, Wang, Boom, & Schutyser, 2015; Wang, de Witt, Schutyser, & Boom, 2014). Extensive laboratory and pilot-plant experimentation is needed for the development of new electrostatic separation applications. The efficiency of the separation process depends on the characteristics of the granular mixtures to be sorted, the feed rate, and the configuration of the electrode (Dascalescu, Tilmatine, Aman, & Mihailescu, 2004).

Optimization of electrostatic separation processes requires the simultaneous control of various electrical and mechanical factors (Dance, Kojovic, & Morrison, 1991; Dascalescu et al., 2004; Iuga, Morar, Samuila, & Dascalescu, 2001). In a roll-type corona–electrostatic separator, for instance, the particles to be separated are fed with a certain speed on the surface of a rotating roll electrode and connected to the ground. A high-intensity electric field is generated between this roll and one or several electrodes connected to a high-voltage supply (Dascalescu, Morar, Iuga, Samuila, & Neamtu, 1998; Iuga, Neamtu, Suarasan, Morar, & Dascalescu, 1998). The insulating particles are charged by ion bombardment in the corona field zone and are pinned to the surface of the rotating roll electrode by the electric image force. The factors influencing the efficiency of the electrostatic separation process include the high-voltage level, the electrode configuration, the feed rate, the particle size, and the roll speed (Dascalescu, Mihalcioiu, et al., 2004).

The design of roll-type corona–electrostatic separator depends on various factors such as roll speed, high voltage amount of corona, and electrostatic electrode that improve the efficiency of process. Tabtabaei, Konakbayeva, Rajabzadeh, and Legge (2019) showed that the functional properties of navy bean protein concentrates obtained by pneumatic triboelectrostatic separation applied a sustainable, chemical-free dry triboelectrostatic separation method for soybean protein concentrate as well as navy bean protein. They reported that the functional properties of these fractions were examined and compared with the commercial soybean protein concentrate as well as navy bean protein isolate obtained by a conventional wet fractionation process. The results showed that protein-enriched fractions had 36–38% protein on a moisture-free basis, accounting for 43% of the total available protein. Analysis of the dry-enriched protein fractions showed a similar protein profile to that of the original navy bean flour. Landauer and Foerst (2018) in a study on the effect of electric field strength and flow rate on the separation of the barley starch and whey protein mix reported that different gas flow rates at a turbulent flow regime in charging tube did not change the separation characteristics. In contrast, increasing electrical field strength increases the separation efficiency of protein particles, regardless of gas flow conditions. The proportion of starch at the anode is the same for all the investigated parameters. Požėlienė, Lynikienė, Šapailaitė, and Sakalauskas (2008) showed that the energy in the corona discharge field appearing in wheat seeds did not affect the relative energy content received by the seed due to the polarization of charge. In the electrostatic separation procedure, the objective of optimization is to increase the efficiency of the process and/or the purity of the products (Dascalescu, Tilmatine, et al., 2004).

The objectives of the present study are as follows: (a) to investigate the effective factors in the electrostatic separation systems using a software environment; (b) to study the behavior of grain and straw particles when moving on surface of a rotary cylindrical electrode and detaching it in an electrostatic field by developing a prototype apparatus, and (c) to do a comparison between simulation and experimental results.

2 | MATERIALS AND METHODS

The straw and wheat grain samples (Mehregan cultivar) were provided from Lorestan Agricultural Research Center. The physical and geometric properties of the particles were measured and their moisture

contents were measured just before the experimental tests using a halogen moisture meter device (PCE-MB-210, PCE, UK), which works based on the gravimetric or loss on drying principle.

2.1 | Experimental procedure

The experiments were performed using a roll-type laboratory electrostatic separator (Carpco Inc., Jacksonville, FL) to study the spatial position of grain and straw particles (Figure 1a). The value of the applied voltage and the rotational speed of the roll-type grounded electrode were the controllable factors to study the performance of separating grain and straw particles in boxes below the apparatus. A schematic view of the electrodes and the trajectory of a particle is shown in Figure 1b. The separator consisted of a vibrating feeder system, a grounded rotating cylinder, a corona wire electrode that was attached to a high voltage supply, and an elliptical electrostatic electrode. Seventeen collecting boxes for grain and straw with 2-cm width were located below the device, covering the entire width of the device. The corona–electrostatic electrodes were connected to a DC voltage supply and fixed at a constant angle of 20 and 60°, respectively, from the perpendicular axis passing through the center of the grounded electrode. The feed rate of particles was passed through a monolayer in the corona electrode zone and was then placed on the grounded electrode. The experiments were performed at three speed levels of a rotating cylinder (50, 70, and 90 rpm) and five voltage levels (10, 15, 20, 25, and 30 kV). The moisture content of grain and straw was 10 and 15%, respectively. The weights of grain and straw were approximately 50 g (±1 g) and 20 g (±1 g), respectively, similar to the ratio of straw and grain weight in a wheat cluster.

The wheat particles were fed at a certain rate by a vibrating mechanism on the surface of a rotating grounded roll electrode in the corona–electrostatic separator. A high-intensity electric field was generated between this roll and the other electrode connected to a DC high-voltage supply. The insulating particles (straw) were charged in the high-voltage field zone and were "pinned" to the surface of the rotating roll electrode because of their low weight while the semi-conductive grain particles were not attracted by the grounded electrode. The electric field strength was the main parameter that affected the behavior of insulating particles, thus the study of the electric field strength distribution is of importance for the design and dimensioning of high-voltage equipment. For each experiment, wheat grain recovery and purity in compartment Bi were calculated, respectively (Richard et al., 2017):

$$\mathrm{REC}_{\mathrm{gBi}} = \frac{m_{\mathrm{gBi}}}{m_{\mathrm{Tg}}} \times 100, \tag{1}$$

$$\mathrm{PUR}_{\mathrm{gBi}} = \frac{m_{\mathrm{gBi}}}{m_{\mathrm{TBi}}} \times 100, \tag{2}$$

where m_{gBi} corresponds to the mass of wheat grain collected in the compartment Bi, m_{Tg} is the total mass of grain in all compartments and is the total wheat grain and straw mass of the compartment Bi. Similar formulas are used to calculate the recovery of straw particles. Since the experimental measurements of the field strength are difficult and are not enough accurate due to the interference of the measuring devices, which may affect the distribution of the electric field, a numerical study was made to define the configuration that might give the best separation. So we used computer-aided methods that can provide us with a good understanding of the process.

2.2 | Mathematical simulation model

During the separation, the charged particles are subjected to an electrostatic force due to the action of the electric field in the inter-electrode zone (Hakima et al. 2017). The distribution of the electric potential U in this area is given by the Laplace equation:

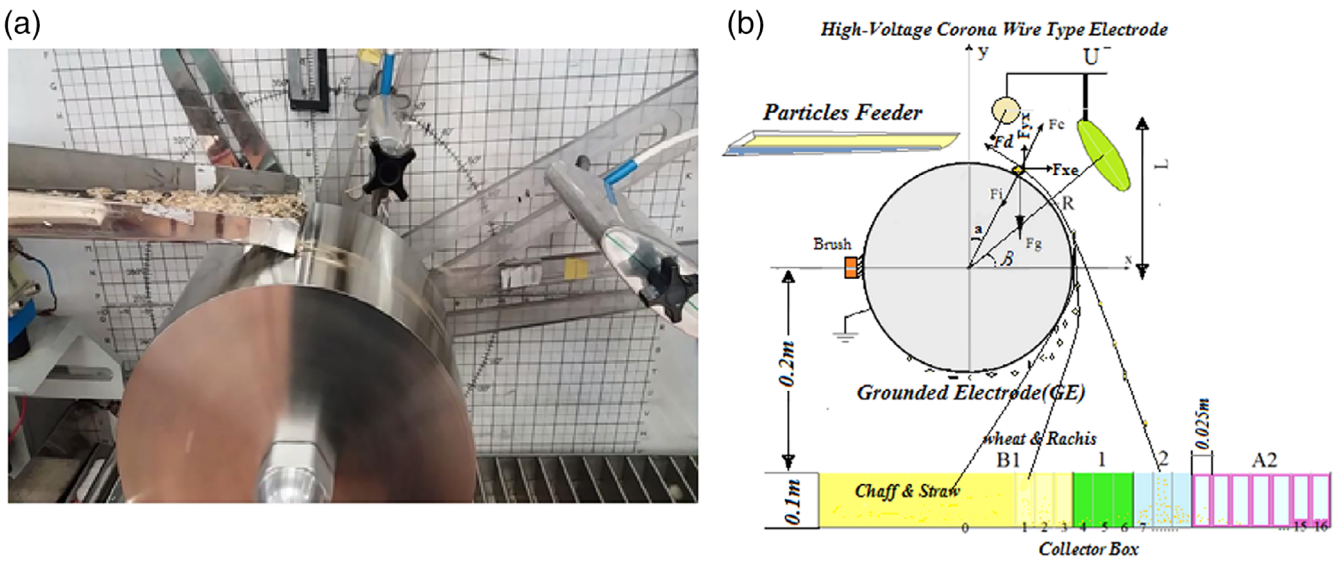

FIGURE 1 (a) Apparatus and (b) schematics for roll-type laboratory electrostatic separator

$$\frac{\partial^2 U}{\partial x^2}+\frac{\partial^2 U}{\partial y^2}+\frac{\partial^2 U}{\partial z^2}=0, \tag{3}$$

$$-\nabla U = E. \tag{4}$$

COMSOL Multiphysics 5a working based on a finite element method can calculate the distribution of the electric field tension in the separation zone using Equation (3). In this study, the geometric position of the electrodes was designed in the COMSOL software environment. After 2D meshing the electric field zone between the electrodes and the boxes, at the specified input voltages, the spatial distribution of electric field intensity was obtained as an output at 25,000 nodes in the field zone. These electric field data along with the rotary speed of the grounded cylinder and the physical properties of the particles entered a code written in the MATLAB 2015 programming environment as the input data. The particles were affected by the mechanical and electrical forces of the separator system including electric image force (F_i), electric field force (F_q), drag force (F_d), gravitational force (F_g), and centrifugal force (F_c) (Figure 2) (Dascalescu et al., 1995; Felice, 1996).

The first step in the path simulation is to determine the departure angle of a moving particle from the surface of a rotating cylinder. The simulation was based on three assumptions (Li, Lu, Xu, & Zhou, 2008): distribution of particles' mass and their movement on the feed path and the cylindrical surface in a monolayer; the space between the particles is high enough so that each particle can be considered independent for examination; and the effect of particles on each other is not significant.

The electrostatic field was simulated in an corona–electrostatic separator system with two corona–electrostatic electrodes in the separation zone. The particles passed through the corona region and were electrically charged. The corona charging equations are as follows (Dascalescu, Mizuno, et al., 1995; Dumitran et al., 2010):

$$\frac{dQ_p}{dt}=\frac{(Q_s-Q_p)^2}{\tau Q_s}, \tag{3}$$

where t is the time, Q_p is corona charging, τ is the time delay constant for particle charging, and Q_s is the saturate corona charging of particle. In addition to the corona charge, the electrical charge induction by the electrostatic field also affects the particles' charge. In total, Q_m, the maximum charge of nonmetallic spherical particle in a constant electric field can be calculated using Equation (2) (Li et al., 2008; Wu, Castle, Inculet, Petigny, & Swei, 2003).

$$Q_m=\frac{0.55d^2\pi\varepsilon_0\varepsilon_r E}{\varepsilon_r+2}. \tag{2}$$

In a corona discharge electric field, a semispherical nonconductive granule of mean diameter d, and relative permittivity ε_r acquire the maximum (saturation) charge Q_s and is calculated by Equation (3) (Li et al., 2008):

$$Q_s=Q_{im}=\pi\varepsilon_0 d^2\left[\frac{3\varepsilon_r}{\varepsilon_r+2}\right]E, \tag{3}$$

where d is the particle mean diameter and E is the electric field tension. In addition, for nonspherical particles, the mean diameter can be obtained using Equation (4)

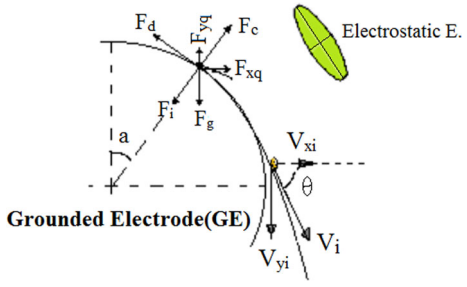

FIGURE 2 Effective forces in the process of particle separation from the rotating cylinder

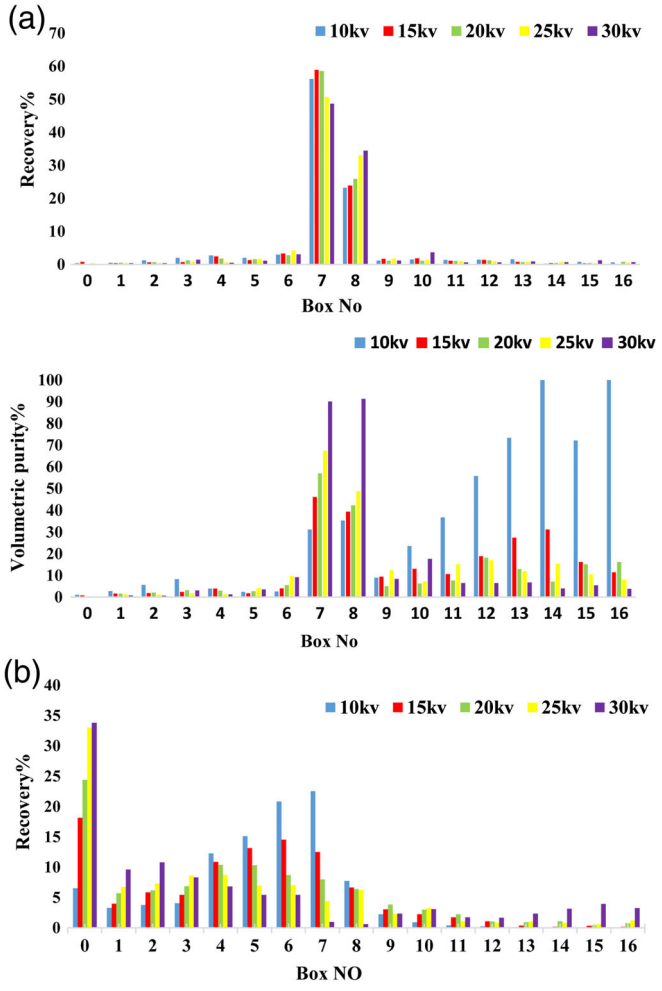

FIGURE 3 Distribution of (a) wheat grain particles (Mc10%), recovery (up)—purity (down) and (b) wheat straw (Mc15%), recovery in collecting boxes in five voltage ranges at 70 rpm

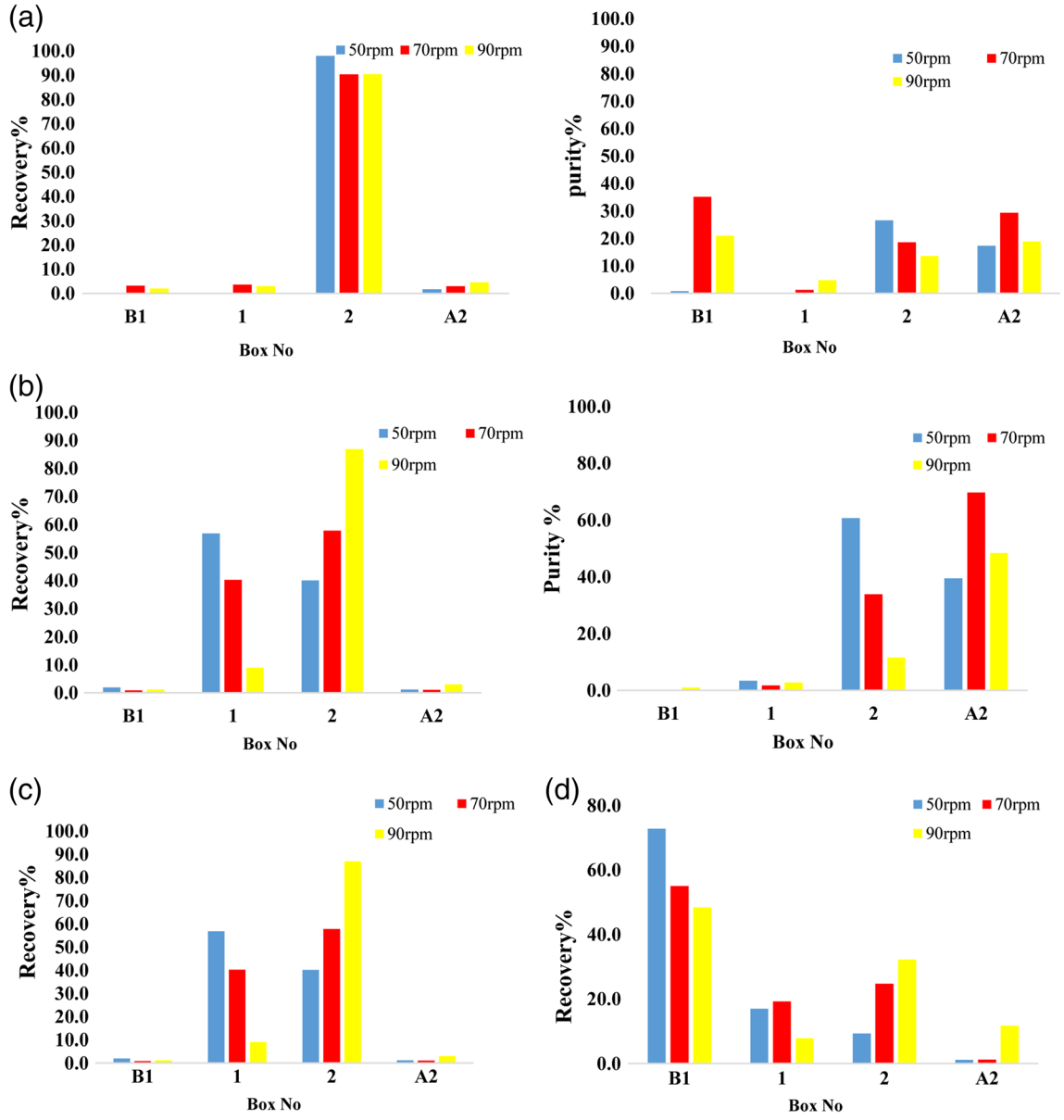

FIGURE 4 Wheat grain particles recovery (left) and purity (right), (a) 5 kV, (b) 25 kV—straw particles recovery, (c) 5 kV, (d) 25 kV

$$d_s = \sqrt{\frac{S_p}{\pi}} = \sqrt{r^2 + 2rh}, \tag{4}$$

where d_s is the mean diameter, S_p is the surface area, and r and h are the maximum radii and thicknesses of the particles, respectively. So, we have the following:

$$Q_s = \pi\varepsilon_0 (r^2 + 2rh)\left[\frac{3\varepsilon_r}{(\varepsilon_r + 2)}\right]E. \tag{5}$$

Particle charging involves induction, one-way neutralization, and corona charge during the process. When the nonconductive particles enter the electric field, they become positively charged (Q_m) because of the positive induction and then, due to the negative corona charging, the positive charge of the particles disappears and then they get negatively charge (Q_s) at saturation. When the time the particles take to pass through the corona zone (t_s) is greater than 5τ, the particles get 95% of their maximum charge (Equation 6) (Iuga et al., 2001)

$$t_s = 5\tau = \frac{20\varepsilon_0\varepsilon_r}{qk}, \tag{6}$$

where q is the charge density in electrical field and k is ion mobility and equal to 2×10^{-4} m^2/V.s. So the necessary time needed for nonconductive particles (t_{gs}) can be calculated by Equation (7)

$$t_{gs} = \frac{60w}{2\pi Rn}, \tag{7}$$

where w is the width of corona zone, R is the radius of the rotating cylinder, and n is the speed of rotation.

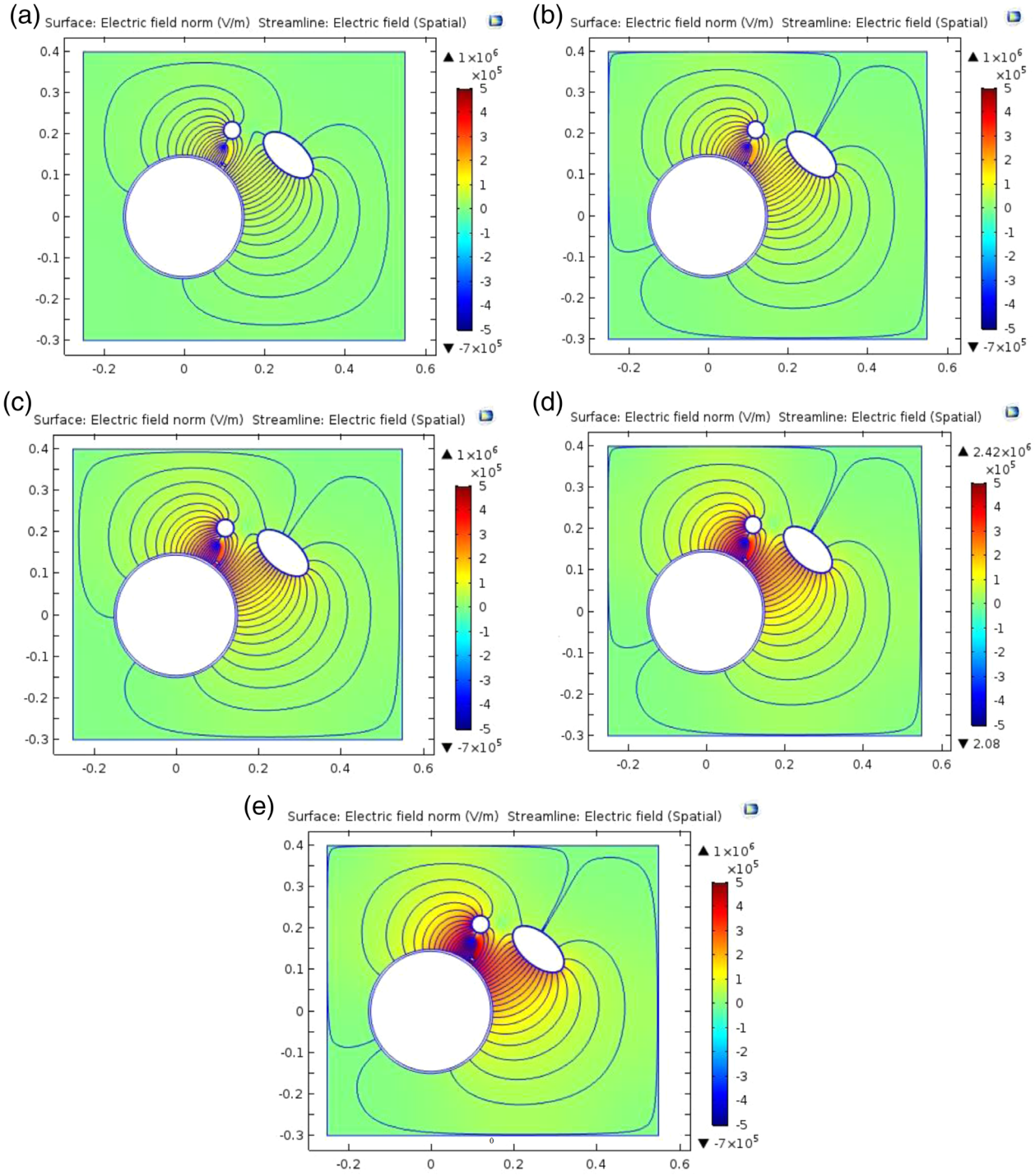

FIGURE 5 Distribution of the norm electric field intensity (V/m) for different voltage levels: (a) 10 kV, (b) 15 kV, (c) 20 kV, (d) 25 kV, and (e) 30 kV

The electric image force F_i that pins the nonconductive granule to the surface of the roll electrode is proportional to the square of the charge Q_i:

$$F_i = \frac{Q_i^2}{\left[4\pi\varepsilon_0 d^2\right]} \le \frac{Q_{im}^2}{\left[4\pi\varepsilon_0 d^2\right]}. \quad (8)$$

These granules will detach from the roll electrode when (Richard et al., 2017)

$$F_e + F_c \ge F_g \cos\alpha_d, \quad (9)$$

$$F_e = |F_q| - F_i, \quad (10a)$$

$$F_q = QE, \quad (10b)$$

where F_c is the centrifugal force, F_g is the gravitational force, and α_d is the detachment angle. For the nonconductive particles such as straw,

detachment usually occurs at $\alpha_d > 180^\circ$, where $E = 0$ and the detachment condition can be simplified (Younes et al., 2007):

$$F_c - F_i > F_g \cos \alpha_d.$$

The Coulombic force (electric attraction) F_e, which in the case of semicylindrical wheat particles, can be expressed as (Salama, Richard, Medles, Zeghloul, & Dascalescu, 2018; Younes et al., 2007):

$$F_e = 0715 Q_d E \text{ before detachment,} \quad (11a)$$

$$F_e = Q_d E \text{ after detachment,} \quad (11b)$$

$$Q_d = 2\pi r_p l \varepsilon_0 E(x_0, y_0), \quad (11c)$$

where $Q_d[C]$ denote the particle charge, E (V/m) is the electric field strength, r_p (m) is the particle radius, l (m) is its length (for semicylindrical wheat grain particle), and ε_0 (F m^{-1}) is the air electric permittivity.

The behavior of the particle separation from the grounded cylinder and its path can be obtained by using Equation (9) (Hong-Zhou, Jia, Jie, & Zhen-Ming, 2006). In nonspherical particles such as wheat or cereal straw, the charge magnitude depends on their surface area. The mean radius (r_s) of the particles can be calculated by using $r_s = \frac{\sqrt{S/\pi}}{3}$, where S is the surface area (Li et al., 2008). At the moment of detaching the particle from the rotating cylinder which is in α angle direction, the force acting on the particle is zero in parallel and perpendicular directions toward the cylinder, and there is no image force (F_i) after this moment. Therefore, we can calculate the angle of particles being detached from the cylindrical surface using Equation (11a–c) (Salama et al., 2018; Younes et al., 2007):

$$F_e + F_g \cos\alpha - F_c = 0 \rightarrow \cos\alpha = \frac{F_c - F_e}{F_g} = 0. \quad (12)$$

The particles' motion in a fluid is faced with the drag force calculated by using Equation (13)

$$F_d = \frac{1}{2}\rho C_d A_p v^2, \quad (13)$$

where F_d denotes the drag force, A_p denotes the particle project area, and v denotes the particle velocity. However, for fine particles in air, F_d is obtained by using the Stokes' equation (Salama et al., 2018)

$$F_d = 6\pi r \eta v, \quad (14)$$

where $\eta = 1.83 \times 10^{-5}$kg/ms was the value considered for the dynamic viscosity of air.

In the whole process, the gravity direction is downward and the centrifugal force is acting on the particle as long as the particle is at the surface of the rotating cylinder:

$$F_g = mg, \quad (15)$$

$$F_c = mR\omega^2 = mR\left(\frac{2\pi n}{60}\right)^2, \quad (16)$$

where m denotes the particle mass. After the particles being detached from the electrode surface, the velocity vector resulting from the outcome of all electrical and mechanical forces determines the angle and initial velocity of the particle in the electric field. All particles of wheat and straw receive electric charge due to the ionization of air with the corona electrodes in proportion to their shape and dielectric properties. Because of receiving more electric charge, straw particles are thrown to the cylinder. In addition, the gravity and centrifugal forces are less than those of grain, and therefore, they are thrown toward the rear of the rotating cylinder and their path is separated from the grain particles path.

The differential equation of particles' motion in the electric field and their acceleration at a point (x_{i-1}, y_{i-1}) are as follows (Younes et al., 2007).

$$\frac{d^2 x_{i-1}}{dt^2} = \frac{\left(F_{qx(i-1)} + F_{dx(i-1)}\right)}{m},$$

$$\frac{d^2 y_{i-1}}{dt^2} = \left(F_{qy(i-1)} + F_{gy(i-1)} + F_{dy(i-1)}\right)/m. \quad (17)$$

The particles' speed at each point (x_i, y_i) can be calculated as follows:

$$v_{xi} = \frac{d^2 x_{i-1}}{dt^2}.t_s + v_{x(i-1)},$$

$$v_{yi} = \frac{d^2 y_{i-1}}{dt^2}.t_s + v_{y(i-1)}. \quad (18)$$

The angle of motion direction with the horizontal axial in each point can be shown as $\alpha = \tan^{-1}\frac{v_{yi}}{v_{xi}}$.

The position of each point can be obtained by the following difference equations:

$$x_{i+1} = v_{xi}.t_s + \frac{1}{2}.\frac{d^2 x_{i-1}}{dt^2}.t_s^2 + x_i,$$

$$y_{i+1} = v_{yi}.t_s + \frac{1}{2}.\frac{d^2 y_{i-1}}{dt^2}.t_s^2 + y_i. \quad (19)$$

3 | RESULTS AND DISCUSSION

3.1 | Experimental results

The experimental results are brought at two parts, that is, for wheat grains and straw particles which are recorded based on their weight in each of the boxes by No. of 0–16 at different applied voltages and rotational speeds.

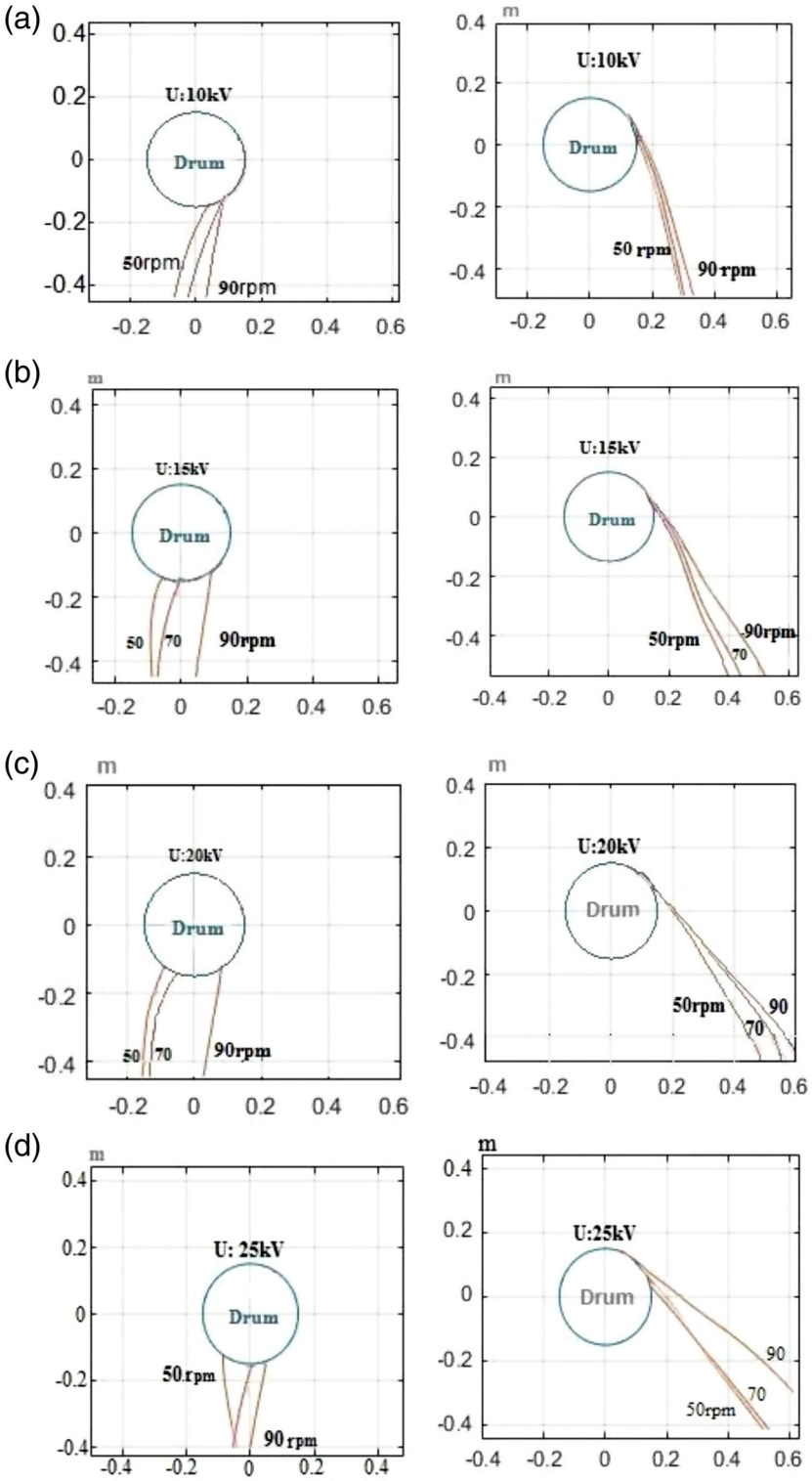

FIGURE 6 Simulated trajectories of wheat grain (right) and straw particles (left) at various rotational speeds of grounded electrode and the applied voltage of a spark discharge (a) 10 kV, (b) 15 kV, (c) 20 kV, and (d) 25 kV between the electrodes

According to Figure 3, an increase in the separating voltage from 10 kV to 30 kV leads to a change in the motion direction of the grain and straw particles toward the electrostatic electrode on the right side of the electric field. Due to the electrostatic electrode repulsion and the image force acting between the grounded electrode and particles, straw particles were thrown to the left boxes. The sticking particles on the surface of the drum are removed by a brush and then they fall into the left boxes.

According to Figure 4, the recovery of grain and straw particles in four box categories (Before1 $_{[0-3]}$, $1_{[4-6]}$, $2_{[7-9]}$, and After2 $_{[10-16]}$) with a width of 300, 75, 75, and 175 mm, respectively, at 5 and 25 kV voltages was compared at three rotational speeds of 50, 70, and 90 rpm.

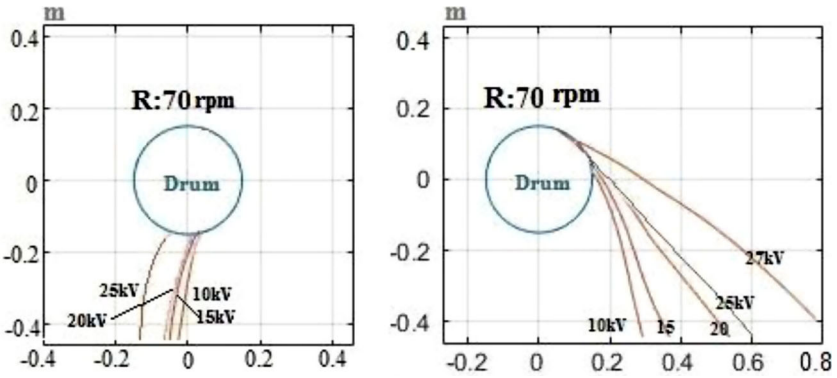

FIGURE 7 Simulated trajectories of wheat grain (right) and straw particles (left) at various applied voltages of a spark discharge (10, 15, 20, 25, and 27 kV) between the electrodes in the 70 rpm rotational speeds of grounded drum electrode

It is observed that an increase in the rotational speed of cylinder from 50 to 90 rpm reduces the effects of increasing the applied voltage from 5 to 25 kV on the particles thrown by the electric field to the boxes located at the right side. An increase in the rotational speed of the cylindrical electrode from 50 to 90 rpm increased the centrifugal force applied to the particles. Eventually, this increase in rotational speed resulted in a change in the path of the grain particle toward the end boxes [A2] and reduced the tendency of straw particles to move toward the primary boxes [B1]. However, the increase in voltage had significant effects on their displacement toward the boxes [2, A2]. Voltage increase led some grain masses to be poured at different boxes, wherein this discrimination was considerably higher at higher rotational speeds. The recovery of grain and straw particles at two voltage levels of 5 and 25 kV was compared, while the rotational speed was set at values of 50, 70, and 90 rpm, respectively. An increase in the rotational speed of the cylindrical electrode from 50 to 90 rpm increased the centrifugal force applied to the particles. Eventually, this increase in rotational speed resulted in a change in the path of the grain particle toward the end boxes [A2] and reduced the tendency of straw particles to move toward the primary boxes [B1]. However, the increase in voltage had significant effects on their displacement toward the end boxes located in the front. Voltage increase from 5 to 25 kV led some grain masses to be poured at different boxes, wherein this discrimination was considerably higher at higher rotational speeds.

By comparison of recovery and volumetric purity of wheat grains and cluster straw due to an increase in voltage from 5 to 25 kV, it was observed that at 5 kV, despite the grain concentration in the box 1 near to the grounded rotating cylinder, the purity was lower than that at the voltage of 25 kV. Separation of grains and straw on the right and left sides of the box was observed with higher volumetric purity and higher quality at all three rotational speeds at a voltage level of 25 kV. In a similar research, at recovery of valuable materials from spent lithium-ion batteries, Silveira et al. (2017) report that the best result was obtained using 25 kV, with 98.24 wt% of metallic materials in conductive fraction.

3.2 | Simulation results

The path of wheat grain and straw particles at different input voltages and cylindrical rotational speeds was simulated using the MATLAB programming software. The effects of voltage magnitude in the form of electric field strength (V/m) for a well-defined configuration of the separator system in two directions of x and y at 28,000 nodes were used in MATLAB program.

The distribution of the magnitude of electric field intensity at different voltage levels is shown in Figure 5. Colledani, Critelli, De Giorgi, and Tasora (2014) obtained similar field intensity results in a simulation of granular particles flowing in electrostatic separation processes at 30 kV voltage.

According to the grain and straw path patterns shown in Figure 6, it is observed that increasing the rotating drum speed from 50 to 70 rpm was effective on the particle shift in all voltage groups, but at 20 kV, an intense path dispersion was observed for both grain and straw particles. The results of practical experiments confirm these findings. It can be concluded that increasing the rotational velocity beyond 70 rpm is not very favorable for better separation of grain from straw particles. Figure 7 reveals that an increase in voltage up to 20 kV for straw and 25 kV for grain particles led to an optimal distribution for separation. However, rotational speeds exceeding 70 rpm lead to particle dispersion and degradation of particle separation quality, so that at 30 kV, simulating the motion of straw particles was impossible and the path of grain particles was capable of being simulated at up to 27 kV and at a speed of 57 rpm. This can be due to the capture and release of particles instantaneously by corona–electrostatic and electrodes at high voltages passing through the electrodes. This phenomenon also was observed in practical experiments. In the study of charged particles trajectories by simulating free-fall electrostatic separators, Labair et al. (2017) showed that an increase of the potential difference ΔU is desired to obtain a good separation. However, an excessive increase of ΔU in the presence of particles characterized by a high Q/m ratio may cause collisions between particles and electrode that affect the quality of the product recovered at separator outlet. It should be noted that excessive increase of ΔU may cause air breakdown in the inter electrode space. In a theoretical simulation and comparison with the experimental results of the aluminum and copper particles separation, Li et al. (2008) obtained a good correlation between computer simulation and practical results at 30 kV voltage. Here as well, similar results were obtained by simulating the rotational electrostatic separator for granular particles at 30 kV and the 70-rpm rotational speed. In a theoretical modeling of

high voltage electrodynamic drum separator, Ciesla (1999a) simulated separating paths and trajectory of healthy and broken grain particles due to their different capacities in electric charging at a voltage of 20 kV and a rotating speed of 76 rpm using a 125 mm radius cylinder. In another research (Ciesla, 1999b), he reported similar experimental results by using a grain particles separator

4 | CONCLUSIONS

The results of practical experiments and simulation in a computer software environment revealed the optimal conditions for separation of wheat straw and grain particles in an electrostatic separation system with a wire-type corona electrode and a 300-mm-diameter cylindrical grounded electrode. The optimum rotational speed was obtained at 70 rpm, and the voltage level required to create the desirable intensity of electric field was in the range of 20–25 kV. Rotational speeds higher than 70 rpm and voltages higher than 25 kV lead to dispersion of wheat straw and grains particles and decrease in the quality of separation.

The results obtained in this study belong to the configuration of the developed prototype with some specifications such as the location of the electrodes. To investigate the effects of these factors, more practical studies should be carried out in future to improve the separation quality.

ACKNOWLEDGMENTS

The practical experiments of this research were carried out in the Lab of Institute of Technology at the University of Poitiers, Angoulême, France, and the authors are thankful to Prof. L. Dascalescu and the members of the laboratory for their contributions to the experiments in the laboratory.

ORCID

Gholamreza Chegini https://orcid.org/0000-0003-1951-1604

REFERENCES

Assatory, A., Vitelli, M., Rajabzadeh, A. R., & Legge, R. L. (2019). Dry fractionation methods for plant protein, starch and fiber enrichment: A review. *Trends in Food Science & Technology*, *86*, 340–351.

Butunoi, T., Buda, G., Dragos, C., Samuila, A., Neamtu, V., Morar, R., … Iuga, A. (2011). Wheat seeds separation in high-intensity electric field. In *2011 7th International Symposium on Advanced Topics in Electrical Engineering (ATEE) (pp. 1–6)*. Bucharest: IEEE.

Ciesla, A. (1999a). New approach to high voltage electrodynamic drum separator. I. Theoretical model. In *11th International Symposium on High Voltage Engineering*, London, England, 425–428.

Ciesla, A. (1999b). New approach to high voltage electrodynamic drum separator. II. Experimental verification. In *11th International Symposium on High Voltage Engineering*, London, England, 406–409.

Colledani, M., Critelli, I., De Giorgi, A., & Tasora, A. (2014). Particle simulation of granular flows in electrostatic separation processes. In The Sixth International Conference on Advances in System Simulation (pp. 203–208).

Dance, A. D., Kojovic, T., & Morrison, R. D. (1991, January). Development of electrostatic separation models for the mineral sands industry. In *AusIMM Extractive Metallurgy Conference (pp. 13–18)*. Australia: Australasian Institute of Mining and Metallurgy.

Dascalescu, L., Mihalcioiu, A. D. R. I. A. N., Tilmatine, A., Mihailescu, M., Iuga, A., & Samuila, A. (2004). Electrostatic separation processes. *IEEE Industry Applications Magazine*, *10*(6), 19–25.

Dascalescu, L., Mizuno, A., Tobazeon, R., Atten, P., Morar, R., Iuga, A., & Samuila, A. (1995). Charges and forces on conductive particles in roll-type corona-electrostatic separators. *IEEE Transactions on Industry Applications*, *31*(5), 947–956.

Dascalescu, L., Morar, R., Iuga, A., Samuila, A., & Neamtu, V. (1998). Electrostatic separation of insulating and conductive particles from granular mixes. *Particulate Science and Technology*, *16*(1), 25–42.

Dascalescu, L., Tilmatine, A., Aman, F., & Mihailescu, M. (2004). Optimization of electrostatic separation processes using response surface modeling. *IEEE Transactions on Industry Applications*, *40*(1), 53–59.

Dascalescu, L., Tobazeon, R., & Atten, P. (1995). Behaviour of conducting particles in corona-dominated electric fields. *Journal of Physics D: Applied Physics*, *28*(8), 1611.

Drintcha, V., Pavlov, S. (2002). Increase of efficiency of seed separation in gravity separator. In *30 Symposium actual tasks of agricultural Engineering*, Opatija, Croatia, 265–273.

Dumitran, L. M., Badicu, L. V., Plopeanu, M. C., & Dascalescu, L. (2010). Efficiency of dual wire-cylinder electrodes used in electrostatic separators. *Revue Roumain Des Sciences Techniques*, *55*(2), 171–180.

Felice, N. J. (1996). Forces et charges de petits object en contat avec une electrode affectee d'un champ electrique. *Rev. General de l'Dlectricite*, *75*, 1145–1160.

Harmond, J. E., Brandenburg, N. R., & Klein, L. M. (1968). Mechanical seed cleaning and handling. In *Agricultural Handbook No: 334*. Agricultural Research: Service. Washington D.C.

Hong-Zhou, L., Jia, L., Jie, G., & Zhen-Ming, X. (2006). Electrostatics of spherical metallic particles in cylinder electrostatic separators/sizers. *Journal of Physics D: Applied Physics*, *39*(18), 4111.

Iuga, A., Morar, R., Samuila, A., & Dascalescu, L. (2001). Electrostatic separation of metals and plastics from granular industrial wastes. *IEE Proceedings-Science, Measurement and Technology*, *148*(2), 47–54.

Iuga, A., Neamtu, V., Suarasan, I., Morar, R., & Dascalescu, L. (1998). Optimal high-voltage energization of corona-electrostatic separators. *IEEE Transactions on Industry Applications*, *34*(2), 286–293.

Kazimirchuk, D. A., & Xziretdinov, V. X. (1995). Dielectric equipment for grading and cleaning of seeds. *Sugar Beet*, *6*(1), 12–13.

Labair, H., Touhami, S., Tilmatine, A., Hadjeri, S., Medles, K., & Dascalescu, L. (2017). Study of charged particles trajectories in free-fall electrostatic separators. *Journal of Electrostatics*, *88*, 10–14.

Landauer, J., & Foerst, P. (2018). Triboelectric separation of a starch-protein mixture–impact of electric field strength and flow rate. *Advanced Powder Technology*, *29*(1), 117–123.

Li, J., Lu, H., Xu, Z., & Zhou, Y. (2008). Critical rotational speed model of the rotating roll electrode in corona electrostatic separation for recycling waste printed circuit boards. *Journal of Hazardous Materials*, *154*(1–3), 331–336.

Li, T. X., Ban, H., Hower, J. C., Stencel, J. M., & Saito, K. (1999). Dry triboelectrostatic separation of mineral particles: A potential application in space exploration. *Journal of Electrostatics*, *47*(3), 133–142.

Messal, S., Zeghloul, T., Benhafssa, A. M., & Dascalescu, L. (2016). Belt-type corona-electrostatic separator for the recovery of conductive and nonconductive products from micronized wastes. *IEEE Transactions on Industry Applications*, *53*(2), 1424–1430.

Miller, B. M., & Copeland, L. (1997). *Seed production: Principles and practices*. New York: International Thomson Publishing.

Mortezapour, H., Moshirirad, S., & Akhbari, M. (2015). Investigating the possibility of removing impurities from saffron sprouts using an electrostatic separator. *Journal of Agricultural Machinery*, *5*(1), 44–51 (in Persian).

Pelgrom, P. J., Wang, J., Boom, R. M., & Schutyser, M. A. (2015). Pre-and post-treatment enhance the protein enrichment from milling and air classification of legumes. *Journal of Food Engineering*, *155*, 53–61.

Požėlienė, A., & Lynikienė, S. (1998). Special cleaning of seeds on the cylindrical electroseparator. *Agricultural Technics*, *35*(5), 6–9.

Požėlienė, A., Lynikienė, S., Šapailaitė, I., & Sakalauskas, A. (2008). Utilization of strong electric field for special cleaning buckwheat seeds. *Agronomy Research*, *6*, 291–298.

Ralston, O. C. (1961). *Electrostatic separation of mixed granular solids (Vol. 9)*. Netherlands: Elsevier Amsterdam.

Rawa, T., & Kaliniewicz, Z. (1998). Effect of selected factors on efficiency of buckwheat seed elevation by wide pocket pits of cylidrical trieur. *Zeszyty Problemowe Postepow Nauk Rolniczych (Poland)*, *4541*, 193–200.

Reguig, A., Bendaoud, A., Dordizadeh, P., Salama, A. R., Messal, S., & Dascalescu, L. (2017). Experimental study of a modified dual-type high-voltage electrode for electrostatic separation applications. *Journal of Electrostatics*, *88*, 232–235.

Remadnia, M., Kachi, M., Messal, S., Oprean, A., Rouau, X., & Dascalescu, L. (2014). Electrostatic separation of peeling and gluten from finely ground wheat grains. *Particulate Science and Technology*, *32* (6), 608–615.

Richard, G., Touhami, S., Zeghloul, T., Salama, A., & Dascalescu, L. (2017). Experimental and numerical evaluation of two electrode systems for plate-type electrostatic separators. *Journal of Electrostatics*, *85*, 1–10.

Salama, A., Richard, G., Medles, K., Zeghloul, T., & Dascalescu, L. (2018). Distinct recovery of copper and aluminum from waste electric wires using a roll-type electrostatic separator. *Waste Management*, *76*, 207–216.

Silveira, A. V. M., Santana, M. P., Tanabe, E. H., & Bertuol, D. A. (2017). Recovery of valuable materials from spent lithium ion batteries using electrostatic separation. *International Journal of Mineral Processing*, *169*, 91–98.

Tabtabaei, S., Jafari, M., Rajabzadeh, A. R., & Legge, R. L. (2016). Solvent-free production of protein-enriched fractions from navy bean flour using a triboelectrification-based approach. *Journal of Food Engineering*, *174*, 21–28.

Tabtabaei, S., Konakbayeva, D., Rajabzadeh, A. R., & Legge, R. L. (2019). Functional properties of navy bean (*Phaseolus vulgaris*) protein concentrates obtained by pneumatic tribo-electrostatic separation. *Food Chemistry*, *283*, 101–110.

Wang, J., de Witt, M., Schutyser, M. A. I., & Boom, R. M. (2014). Analysis of electrostatic powder charging for fractionation of foods. *Innovative Food Science and Emerging Technologies*, *26*, 360–365.

Wu, Y., Castle, G. P., Inculet, I. I., Petigny, S., & Swei, G. (2003). Induction charge on freely levitating particles. *Powder Technology*, *135*, 59–64.

Younes, M., Tilmatine, A., Medles, K., Rahli, M., & Dascalescu, L. (2007). Numerical modeling of conductive particle trajectories in roll-type corona-electrostatic separators. *IEEE Transactions on Industry Applications*, *43*(5), 1130–1136.

How to cite this article: Jafari M, Chegini G, Shayegani Akmal AA, Rezaeealam B. A roll-type corona discharge–electrostatic separator for separating wheat grain and straw particles. *J Food Process Eng*. 2019;e13281. https://doi.org/10.1111/jfpe.13281